η-exponents in the one-dimensional antiferromagnetic Heisenberg model with next-nearest-neighbour coupling

1997 J. Phys.: Condens. Matter 9 3435

(http://iopscience.iop.org/0953-8984/9/16/015)

J. Phys.: Condens. Matter **9** (1997) 3435–3445. Printed in the UK PII: S0953-8984(97)81012-0

η-exponents in the one-dimensional antiferromagnetic Heisenberg model with next-nearest-neighbour coupling

C Gerhardt†, A Fledderjohann†, E Aysal†, K-H Mütter†§, J F Audet‡ and H Kröger‡

† Physics Department, University of Wuppertal, 42097 Wuppertal, Germany
‡ Department of Physics, Université Laval, Quebec, Quebec G1K 7P4, Canada

Received 16 January 1997

Abstract. We investigate the critical exponents $\eta_3(\alpha, M)$ and $\eta_1(\alpha, M)$ associated with the singularities in the longitudinal and transverse structure factors of the one-dimensional antiferromagnetic Heisenberg model with nearest- (J_1-) and next-nearest- (J_2-) neighbour coupling of relative strength $\alpha = J_2/J_1$ and an external field B with magnetization $M(B)$.

1. Introduction

In this paper we are going to study the critical behaviour in the one-dimensional spin-$\frac{1}{2}$ antiferromagnetic Heisenberg model

$$H = 2\sum_{x=1}^{N}(\boldsymbol{S}(x)\cdot\boldsymbol{S}(x+1) + \alpha\boldsymbol{S}(x)\cdot\boldsymbol{S}(x+2)) - 2B\sum_{x=1}^{N} S_3(x) \tag{1.1}$$

with next-nearest-neighbour coupling α and external field B. The phase structure in the absence of an external field ($B = 0$) has been studied intensively before [1–11]. Let us briefly summarize those results relevant for our later investigation. The ground state of the model is a singlet ($S = 0$) state with momentum p_0, where $p_0 = 0$ for $N = 4, 8, 12, \ldots$ and $p_0 = \pi$ for $N = 6, 10, 14, \ldots$. This statement holds for $\alpha < \frac{1}{2}$. At $\alpha = \frac{1}{2}$ the model reduces to the Majumdar–Ghosh model [10] with degenerate dimer ground states.

The quantum numbers of the first excited state change with α: there is a triplet ($S = 1$) state for $0 < \alpha < \alpha_c$ and a singlet ($S = 0$) state for $\alpha_c < \alpha < \frac{1}{2}$. α_c marks the transition from the gapless 'spin-fluid' phase ($\alpha < \alpha_c$) to the 'dimer' phase ($\alpha > \alpha_c$) with a gap. The most precise value for $\alpha_c = 0.241\,167$ has been reported recently by Eggert [11]. The structure of these two phases can be explored by means of the static and dynamical correlation functions of appropriate operators. In the spin-fluid phase where $0 < \alpha < \alpha_c$ the $\Delta S = 1$ operator

$$S_3(p) = \frac{1}{\sqrt{N}}\sum_{x=1}^{N} \mathrm{e}^{\mathrm{i}px} S_3(x) \tag{1.2}$$

§ e-mail: muetter@wpts0.physik.uni-wuppertal.de.

0953-8984/97/163435+11$19.50

generates the transition from the singlet to the triplet excited state. To examine the dimer phase where $\alpha > \alpha_c$ we need a $\Delta S = 0$ operator. These transitions are generated by the dimer operator

$$D(p) = \frac{1}{\sqrt{N}} \sum_{x=1}^{N} e^{ipx} (\boldsymbol{S}(x) \cdot \boldsymbol{S}(x+1) - \langle \boldsymbol{S}(x) \cdot \boldsymbol{S}(x+1) \rangle). \tag{1.3}$$

The corresponding static structure factors

$$S_3(\alpha, p, N) = \langle S_3^+(p) S_3(p) \rangle \qquad \text{and} \qquad D(\alpha, p, N) = \langle D^+(p) D(p) \rangle \tag{1.4}$$

behave as follows for $N \to \infty$. $S_3(\alpha, p = \pi, N)$ diverges logarithmically for $\alpha \leqslant \alpha_c$ but stays finite for $\alpha > \alpha_c$. $D(\alpha, p = \pi, N)$ diverges with a power law depending on α for $\alpha > \alpha_c$ and stays finite for $\alpha < \alpha_c$. The power behaviour changes to a logarithmic behaviour for $\alpha = \alpha_c$.

In the presence of an external field B the ground state of the model has total spin $S = MN$, where $M = M(\alpha, B)$ is the magnetization. The behaviour of the magnetization curve $M(\alpha, B)$ near saturation ($B \to B_s$, $M \to \frac{1}{2}$) changes with α [12].

At $\alpha = 0$ it is known to develop a square-root singularity [13]:

$$M(\alpha = 0, B) \to \frac{1}{2} - \frac{1}{\pi}(B_s - B)^{1/2} \qquad \text{for } B \to B_s \tag{1.5}$$

whereas the numerical data for $\alpha = \frac{1}{4}$ ($N \leqslant 28$) support a quartic-root singularity for $\alpha = \frac{1}{4}$ [12]:

$$M\left(\alpha = \frac{1}{4}, B\right) \to \frac{1}{2} - \frac{1}{2\epsilon_4^{1/4}}(B_s - B)^{1/4} \qquad \epsilon_4 = 1.70(5) \qquad \text{for } B \to B_s. \tag{1.6}$$

The gap in the dimer phase $\alpha > \alpha_c$ appears in the weak-field behaviour of the magnetization curve:

$$M(\alpha, B) \to 0 \qquad B < B_c(\alpha) \qquad \alpha > \alpha_c. \tag{1.7}$$

Note that the model with $B > B_c(\alpha)$ is gapless, provided that there are no 'plateaus' ($M(\alpha, B) =$ constant for $B_{1c} \leqslant B \leqslant B_{2c}$) in the magnetization curve.

The momentum of the ground state p_S follows Marshall's sign rule [14]:

$$\begin{aligned} p_S &= 0 \qquad \text{for } 2S + N = 4n \\ p_S &= \pi \qquad \text{for } 2S + N = 4n + 2 \end{aligned} \tag{1.8}$$

for $0 < \alpha < \frac{1}{4}$.

The singularities in the static structure factors change if we switch on an external field: the transverse structure factor at $p = \pi$

$$S_1(\alpha, p = \pi, M, N) \approx B_1(\alpha, M) N^{1-\eta_1(\alpha, M)} + A_1(\alpha, M) \tag{1.9}$$

diverges with a field-dependent critical exponent $\eta_1(\alpha, M)$. $\eta_1(\alpha = 0, M)$ has been calculated in [15] by means of the Bethe *ansatz*. A second, weaker singularity, which moves with the external field, appears at the soft-mode momentum $p = p_1(M) = 2\pi M$. To our knowledge, the positions of both singularities are independent of α. The critical exponent $\eta_1(\alpha, M)$, however, does depend on α. It has been found to take the values [16]

$$\eta_1\left(\alpha = 0, M = \frac{1}{4}\right) = 0.65(2) \qquad \text{and} \qquad \eta_1\left(\alpha = \frac{1}{4}, M = \frac{1}{4}\right) = 1.16(2). \tag{1.10}$$

The longitudinal structure factor at $p = \pi$ ($M > 0$) stays finite for $\alpha < \frac{1}{4}$ but develops a singularity at the field-dependent soft-mode momentum $p = p_3(M) = \pi(1 - 2M)$:

$$S_3(\alpha, p = p_3(M), M, N) \approx B_3(\alpha, M)N^{1-\eta_3(\alpha,M)} + A_3(\alpha, M). \tag{1.11}$$

Again, the position of the singularity does not depend on α, whereas the critical exponent $\eta_3(\alpha, M)$ changes drastically with α:

$$\eta_3\left(\alpha = 0, M = \frac{1}{4}\right) = 1.50 \qquad \text{and} \qquad \eta_3\left(\alpha = \frac{1}{4}, M = \frac{1}{4}\right) = 0.84. \tag{1.12}$$

The soft-mode singularity at $p = p_3(M)$ is also found in the dimer structure factor $D(\alpha, p, N)$ defined in (1.3) and (1.4). A finite-size analysis of the type (1.11) for $D(\alpha, p, N)$ yields for the critical exponents [16]

$$\eta_D\left(\alpha = 0, M = \frac{1}{4}\right) = 1.49 \qquad \text{and} \qquad \eta_D\left(\alpha = \frac{1}{4}, M = \frac{1}{4}\right) = 0.82. \tag{1.13}$$

These values almost coincide with those of the longitudinal structure factor given in (1.12).

It is the purpose of this paper to determine the complete α-dependence of the critical exponents $\eta_1(\alpha, M)$, $\eta_3(\alpha, M)$.

The paper is organized as follows. In section 2 we explore the range of validity of Marshall's sign rule (1.8). In section 3 we study the impact of the next-nearest-neighbour coupling on the low-lying excitations and on the static structure factors. The latter are computed numerically for system sizes up to $N = 32$. A finite-size analysis of (1.9) and (1.11) yields the critical exponents $\eta_1(\alpha, M)$, $\eta_3(\alpha, M)$. Section 4 is devoted to the study of an unexpected phenomenon, which we found for negative α-values: for $\alpha < \alpha_-(M)$ the finite-size behaviour of the longitudinal structure factor (1.11) changes systematically from a monotonic increase to a decrease.

2. The impact of frustration on the ground states; level crossings

It was pointed out in the introduction that the momenta $p_S(\alpha)$ of the ground states $|S, S_z = S, p_S(\alpha)\rangle$ in the sectors with total spin S follow Marshall's sign rule for $\alpha \leqslant \frac{1}{4}$. We found deviations from this rule for

$$\alpha > \alpha_0(M). \tag{2.1}$$

We computed the ground-state energies $E(\alpha, p_S(\alpha), M, N)$ for small systems with $N = 10, \ldots, 20$ sites. The dependence on the frustration parameter α is shown in figure 1 for $N = 12$. Here we have marked the different ground-state momenta with different symbols.

At $M = S/N = 0$, deviations from Marshall's sign rule occur first at

$$\alpha_0(M = 0) = \frac{1}{2}. \tag{2.2}$$

Here we meet the Majumdar–Ghosh model [10], which is known to have two degenerate ground states, namely dimer states with momenta $p = 0$ and $p = \pi$.

A twofold degeneracy—with respect to the ground-state momenta $p_S^{(1)}(\alpha)$ and $p_S^{(2)}(\alpha)$—emerges along the whole curve $\alpha = \alpha_0(M)$, which is plotted for $N = 10, \ldots, 20$ in figure 2.

The first momentum of the ground state, $p_S^{(1)}(\alpha_0)$, follows Marshall's sign rule (1.8). We have looked for an empirical rule for the second momentum, $p_S^{(2)}(\alpha_0)$, but we did not find such a rule which holds for all momenta and system sizes N.

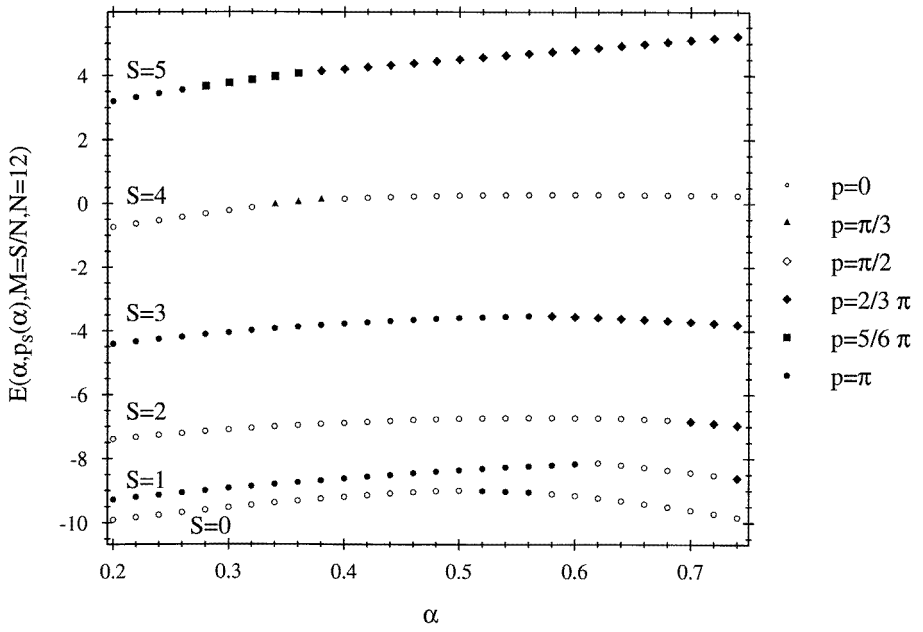

Figure 1. The ground-state energies $E(\alpha, p_S, M = S/N, N)$ in the sector with total spin S on a ring with $N = 12$ sites. The ground-state momenta $p_S(\alpha)$ change with the next-nearest-neighbour coupling α as indicated by the different symbols.

In the saturating-field limit $M \to \frac{1}{2}$, the curve $\alpha_0(M)$ meets the point

$$\alpha_0\left(M \to \frac{1}{2}\right) = \frac{1}{4}. \tag{2.3}$$

Indeed, the eigenvalue problem can be solved analytically for $S = N/2 - 1$ with the *ansatz* (one-magnon states)

$$\left|p, S = \frac{N}{2} - 1\right\rangle = \frac{1}{\sqrt{N}} \sum_x \mathrm{e}^{\mathrm{i}px} |x\rangle \tag{2.4}$$

where $|x\rangle$ denotes a spin state with spin $-\frac{1}{2}$ at site x and spin $\frac{1}{2}$ at all other sites. The energy of the one-magnon state is found to be

$$E\left(\alpha, p, M = \frac{1}{2} - \frac{1}{N}, N\right) = 2\cos p + 2\alpha\cos(2p) + \left(\frac{N}{2} - 2\right)(1 + \alpha). \tag{2.5}$$

The ground-state energy and its momentum $p = p_S(\alpha)$ follow by minimizing (2.5) with respect to p. For $\alpha < \frac{1}{4}$ the ground-state momentum is found to be $p_S^{(1)}(\alpha) = \pi$, $S = N/2 - 1$, in accord with Marshall's sign rule. For $\alpha > \frac{1}{4}$, however, the minimum is found for $p = p_S^{(2)}(\alpha)$ where

$$\cos p_S^{(2)}(\alpha) = -\frac{1}{4\alpha} \qquad S = \frac{N}{2} - 1 \qquad N \to \infty. \tag{2.6}$$

On finite lattices, the difference between the two momenta turns out to be

$$\Delta p_S\left(\alpha_0 = \frac{1}{4}\right) = \left|p_S^{(1)}\left(\alpha_0 = \frac{1}{4}\right) - p_S^{(2)}\left(\alpha_0 = \frac{1}{4}\right)\right| = \frac{2\pi}{N} \qquad S = \frac{N}{2} - 1. \tag{2.7}$$

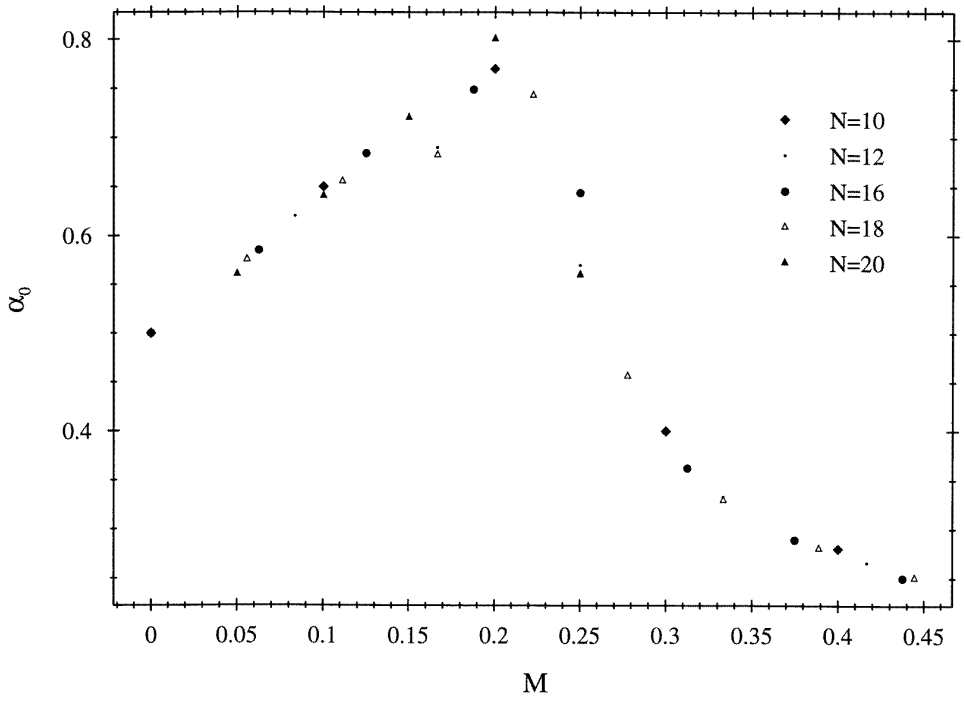

Figure 2. The curve $\alpha = \alpha_0(M = S/N)$, where the ground state $|S, p\rangle$ in the sector with total spin S is degenerate with respect to the momentum $p = p_S^{(1)}(\alpha), p_S^{(2)}(\alpha)$.

As a consequence of the level crossing at $\alpha = \alpha_0(M = S/N)$, M fixed, the derivatives of the ground-state energies

$$\frac{\partial}{\partial\alpha} E\left(\alpha, p_S(\alpha), M = \frac{S}{N}, N\right) \tag{2.8}$$

change discontinuously, as can be seen in an enlargement of figure 1.

3. Soft modes in the excitation spectrum and the associated η-exponents

We have studied the finite-size dependence of the energy gaps

$$\omega_{\Delta S}(\alpha, p, M, N) = E\left(\alpha, p_S + p, M = \frac{S + \Delta S}{N}, N\right) - E\left(\alpha, p_S, M = \frac{S}{N}, N\right) \tag{3.1}$$

for $\Delta S = 0$ and $\Delta S = 1$ in the domain $\alpha < \alpha_0(M)$ where the ground-state momentum p_S follows Marshall's sign rule. In this regime the gap $\omega_{\Delta S=1}(\alpha, p = \pi, M, N)$ vanishes in the thermodynamical limit in such a way that the scaled quantity

$$\lim_{N\to\infty} N\omega_{\Delta S=1}(\alpha, p = \pi, M, N) = \Omega_1(\alpha, M) \qquad \alpha < \alpha_0(M) \tag{3.2}$$

converges to a finite non-vanishing limit. The same holds for the gap $\omega_{\Delta S=0}(\alpha, p = p_3(M), M, N)$, $p_3(M) = \pi(1 - 2M)$, if the next-nearest-neighbour coupling α is positive:

$$\lim_{N\to\infty} N\omega_{\Delta S=0}(\alpha, p = p_3(M), M, N) = \Omega_3(\alpha, M). \tag{3.3}$$

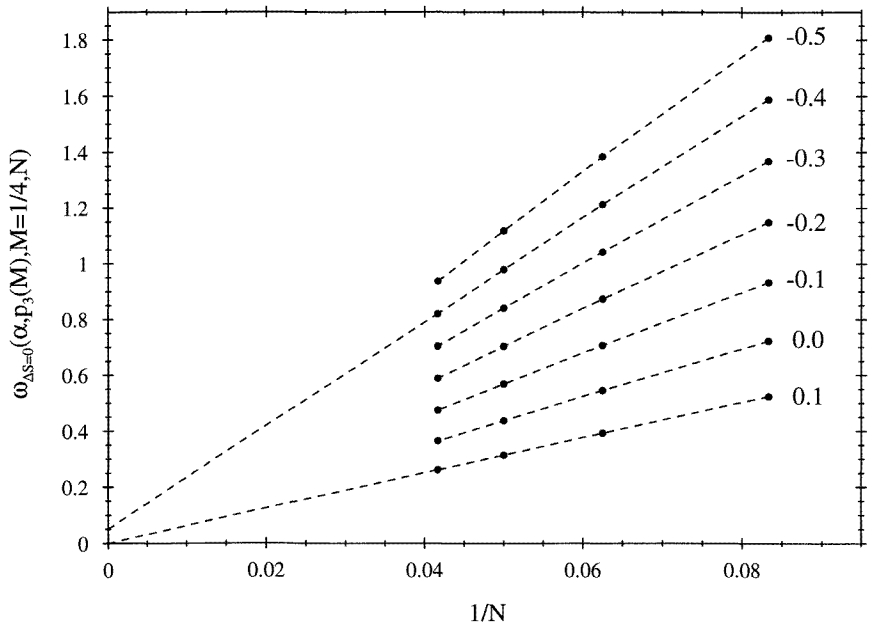

Figure 3. The finite-size dependence of the gap $\omega_{\Delta S=1}(\alpha, p_3(M), M, N)$ for $\alpha = 0.1, 0.0, -0.1, -0.2, -0.3, -0.4, -0.5$.

For negative α-values ($\alpha < \alpha_-(M) < 0$), however, we observe a tendency in the numerical data which at least hints at the emergence of a gap at the momentum $p = p_3(M)$:

$$\lim_{N\to\infty} \omega_{\Delta S=0}(\alpha, p = p_3(M), M, N) = \Delta_3(\alpha, M) \qquad \alpha < \alpha_-(M) < 0 \tag{3.4}$$

as can be seen from figure 3. It is hard to decide from the finite-system results (where $N = 16, 20, 24$) the exact position $\alpha = \alpha_-(M)$ at which the gap (3.4) opens.

In the gapless regimes, where (3.2) and (3.3) are valid, we expect that the critical behaviour of the system is properly described by conformal field theory [17]. This means in particular that the ratios

$$2\theta_a(\alpha, M) = \frac{\Omega_a(\alpha, M)}{\pi v(\alpha, M)} \qquad a = 3, 1 \tag{3.5}$$

can be identified with the critical exponents $\eta_a(\alpha, M)$ [18–20]:

$$2\theta_a(\alpha, M) = \eta_a(\alpha, M) \qquad a = 1, 3. \tag{3.6}$$

Here

$$v(\alpha, M) = \frac{1}{2\pi} \lim_{N\to\infty} N\left(E\left(\alpha, p = p_S + \frac{2\pi}{N}, M = \frac{S}{N}, N\right) - E\left(\alpha, p_S, M = \frac{S}{N}, N\right)\right) \tag{3.7}$$

is the spin-wave velocity. For fixed values of M ($M = \frac{1}{6}, \frac{1}{4}, \frac{1}{3}$) we have determined the α-dependence of $2\theta_a(\alpha, M), a = 1, 3$, from the energy differences (3.1) and (3.7) as they enter in the ratios (3.5). The result can be seen from the solid curves in figures 4(a), 4(b), 4(c). The solid dots represent the determination of the critical exponents $\eta_1(\alpha, M), \eta_3(\alpha, M)$ as they follow from a fit of the form (1.9), (1.11) to the finite-system results ($N \leqslant 32$). Comparing the two determinations we come to the following conclusions.

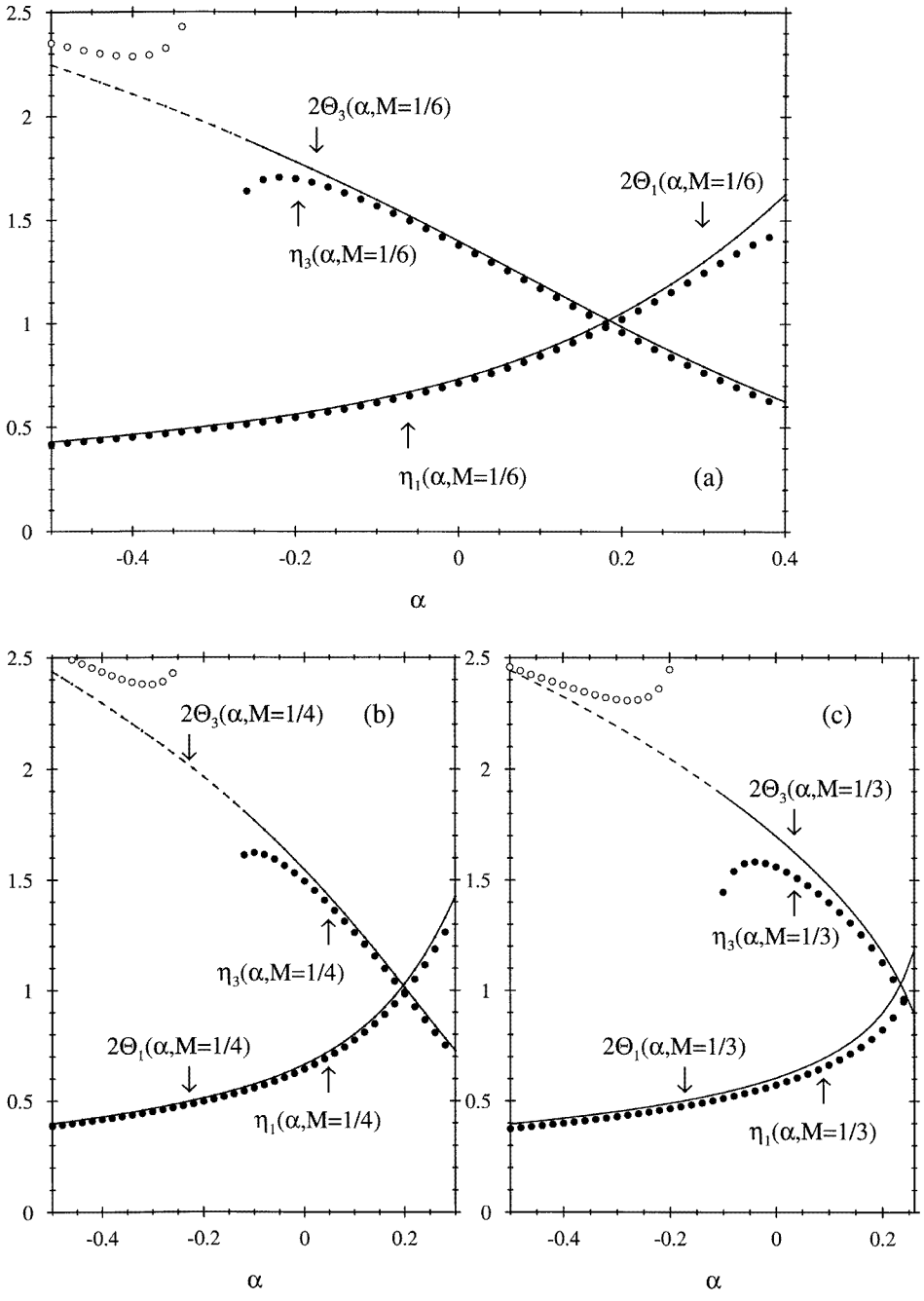

Figure 4. Comparison of the ratio $2\theta_i(\alpha, M), i = 1, 3$, equation (3.5) (solid curves), and the critical exponents $\eta_i(\alpha, M), i = 1, 3$, in the static structure factors given by equations (1.9) and (1.11). (a) $M = \frac{1}{6}$, (b) $M = \frac{1}{4}$, (c) $M = \frac{1}{3}$. Open symbols for $\eta_3(\alpha, M)$ and dashed symbols for $2\theta_3(\alpha, M)$ have been used for $\alpha < \alpha_-(M)$, where we expect a breakdown of the finite-size *ansatz* (1.11).

(i) The identity $2\theta_1(\alpha, M) = \eta_1(\alpha, M)$ for the critical exponent in the transverse structure factor is well established for $-0.5 < \alpha < 0.25$.

The same holds for the identity $2\theta_3(\alpha, M) = \eta_3(\alpha, M)$ for the critical exponent in the longitudinal structure factor in the interval $0 < \alpha < 0.25$. If we approach the curve $\alpha = \alpha_0(M)$, the convergence of the Lanczos algorithm slows down more and more, due to the emergence of the level crossing discussed in section 2.

(ii) The two curves $2\theta_1(\alpha, M)$, $2\theta_3(\alpha, M)$ cross each other at $\alpha = \alpha_c(M)$:

$$2\theta_1(\alpha_c(M), M) = 2\theta_3(\alpha_c(M), M) = 2\theta(M) \tag{3.8}$$

where

$$\alpha_c\left(M = \frac{1}{6}\right) = 0.18 \qquad \alpha_c\left(M = \frac{1}{4}\right) = 0.20 \qquad \alpha_c\left(M = \frac{1}{3}\right) = 0.24 \tag{3.9}$$

and

$$2\theta\left(M = \frac{1}{6}\right) = 1.01 \qquad 2\theta\left(M = \frac{1}{4}\right) = 1.02 \qquad 2\theta\left(M = \frac{1}{3}\right) = 1.02. \tag{3.10}$$

The α-values are quite close to the point of the transition $\alpha_c(M = 0) = 0.241$ from the spin fluid to the dimer phase. The same holds for the critical exponents $\eta(M)$, which deviate only slightly from $\eta(M = 0) = 1$.

(iii) The relation

$$4\theta_1(\alpha, M)\theta_3(\alpha, M) = 1 \tag{3.11}$$

appears to be satisfied within a few per cent for $0 \leqslant \alpha \leqslant \frac{1}{4}$.

(iv) For negative values of α, the ratio $2\theta_3(\alpha, M)$ is smooth, whereas the results for $\eta_3(\alpha, M)$ seem to develop a discontinuous structure. We suggest, that this is an artefact of the simple *ansatz* (1.11), which is no longer able to adequately describe the finite-size dependence of the longitudinal structure factor. Surprisingly enough, the latter changes drastically with α.

For $\alpha > \alpha_-(M)$,

$$\alpha_-\left(M = \frac{1}{6}\right) = -0.31 \qquad \alpha_-\left(M = \frac{1}{4}\right) = -0.19 \qquad \alpha_-\left(M = \frac{1}{3}\right) = -0.15 \tag{3.12}$$

the longitudinal structure factor increases monotonically with N, whereas it decreases for $\alpha < \alpha_-(M)$. In the latter regime we expect the emergence of the gap (3.4).

4. The disappearance of a field-dependent soft mode

The changes in the finite-size dependence of the gap (3.3), (3.4), and of $S_3(\alpha, p_3(M), M, N)$ provide us with a first hint that the field-dependent soft mode at $p = p_3(M) = \pi(1 - 2M)$ might disappear for $\alpha < \alpha_-(M)$. In this section, we are looking for further evidence for this hypothesis. In figures 5(a), 5(b) we compare the momentum distribution of $S_3(\alpha, p, M = \frac{1}{4}, N)$ for $\alpha = \alpha_-(M = \frac{1}{4}) = -0.19$ and $\alpha = -0.4$, respectively. At $\alpha = \alpha_-(M = \frac{1}{4}) = -0.19$ (figure 5(a)) the momentum distribution is well approximated by two straight lines with different slopes for $p < p_3(M)$ and $p > p_3(M)$, respectively. This discontinuity is more and more washed out if the next-nearest-neighbour coupling decreases further. For example, at $\alpha = -0.4$ (figure 5(b)) the p-distribution of the longitudinal structure factor appears to be smooth in the thermodynamic limit. The approach to this limit is indicated by an arrow. $S_3(\alpha, p, M, N), \alpha \leqslant \alpha_-(M)$, is monotonically decreasing with N for $p \leqslant p_3(M)$ but increasing for $p > p_3(M)$.

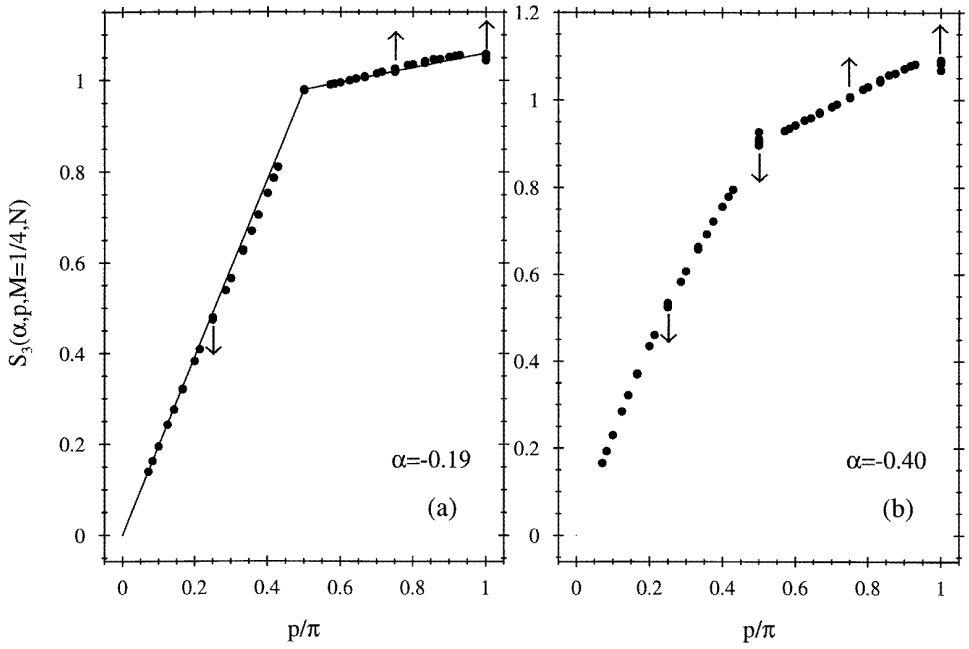

Figure 5. The momentum dependence of the longitudinal structure factor $S_3(\alpha, p, M = \frac{1}{4}, N)$, $N = 28, 24, 20, \ldots$. (a) $\alpha = \alpha_-(M = \frac{1}{4}) = -0.19$, (b) $\alpha = -0.40$.

A more drastic effect can be seen in the dynamical structure factor:

$$S_3(\alpha, \omega, p, M, N) = \sum_n \delta(\omega - (E_n - E_s))|\langle n|S_3(p)|S\rangle|^2 \tag{4.1}$$

which we computed by means of the recursion method [21, 22] for $M = \frac{1}{4}$ and $N = 28$. Here E_s and E_n denote the energies in the ground state $|S\rangle$ with total spin S and the excited states $|n\rangle$. The excitation spectrum is plotted in figures 6(a), 6(b) for $\alpha = -0.19$ and $\alpha = -0.4$, respectively. The numbers denote the corresponding relative spectral weight in percentage terms. Open symbols represent excitations with a relative spectral weight less than 10%. The curves guide the eye to the excitations with dominant spectral weight. For $\alpha = -0.19$ (figure 6(a)) the spectral weight is distributed over a band of excitation energies which broadens in the vicinity of the momentum $p = p_3(M)$. For $\alpha = -0.4$ (figure 6(b)), however, the spectral weight is more concentrated at higher excitation energies. In particular, the lowest excitation at $p = p_3(M)$ has a relative spectral weight less than 10% for $N = 28$.

5. Discussion and conclusion

In this paper, we have studied the impact of a next-nearest-neighbour coupling α and an external field B on the zero-temperature properties of the one-dimensional spin-$\frac{1}{2}$ antiferromagnetic Heisenberg model. We found the following features.

(i) The momentum of the ground state follows Marshall's sign rule (1.8) for $\alpha \leqslant \alpha_0(M)$ where $\alpha_0(0) = \frac{1}{2}$ and $\alpha_0(\frac{1}{2}) = \frac{1}{4}$. The ground state is twofold degenerate with respect to its momentum for $\alpha = \alpha_0(M)$.

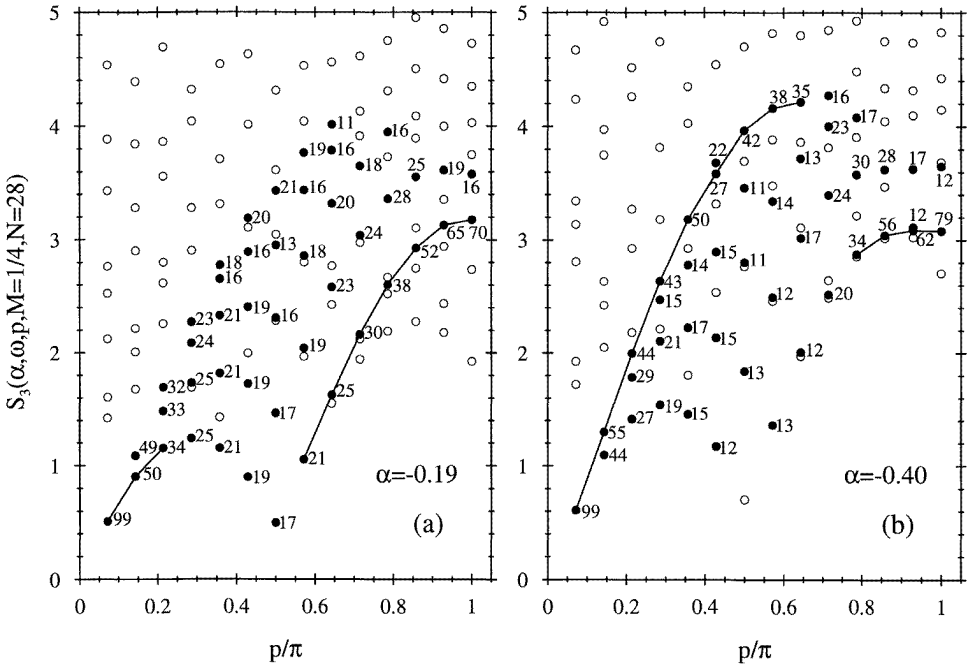

Figure 6. Excitation energies and relative spectral weights in the dynamical structure factor $S_3(\alpha, \omega, p, M = \frac{1}{4}, N = 28)$ in percentage terms. The lines connect the excitations with the dominant spectral weight. (a) $\alpha = \alpha_-(M = \frac{1}{4}) = -0.19$, (b) $\alpha = -0.4$.

(ii) A study of the finite-size dependences (1.9) and (1.11) yields the α-dependence of the critical exponents $\eta_1(\alpha, M), \eta_3(\alpha, M)$ associated with the soft-mode singularities at $p = \pi$ and $p = p_3(M)$ in the transverse and longitudinal structure factor, respectively. Good agreement is found with the prediction (3.5), (3.6) of conformal field theory for $\eta_1(\alpha, M)$ when $-\frac{1}{2} < \alpha < \frac{1}{4}$ and for $\eta_3(\alpha, M)$ when $0 < \alpha < \frac{1}{4}$ (figures 4(a)–4(c)). For these α-values the spectral weight—entering into the definition of the corresponding dynamical structure factors (4.1)—is concentrated around the lower bound of the excitation spectrum. This seems to be a crucial condition for the critical behaviour to be described correctly by conformal field theory. In the thermodynamical limit the dynamical structure factors $S_1(\alpha, \omega, p = \pi, M)$ and $S_3(\alpha, \omega, p = p_3(M), M)$ develop infrared singularities $\omega^{-(2-\eta_a(\alpha))}, a = 1, 3$, which can clearly be seen in a finite-size scaling analysis. Such an analysis was performed in [15] for $\alpha = 0$.

(iii) Deviations from the relation (3.6)—predicted by conformal field theory—appear in the longitudinal case where $a = 3$ (figures 4(a)–4(c)) for negative values of the next-nearest-neighbour coupling and increasing M-values. This is accompanied by the fact that the spectral weight in (4.1) is distributed over a band of excitation energies, which broadens with decreasing values of α.

(iv) There are several indications that the field-dependent soft mode at $p = p_3(M) = \pi(1-2M)$ disappears for negative next-nearest-neighbour couplings $\alpha < \alpha_-(M) < 0$: a gap (3.4) opens and the longitudinal structure factor (1.11) changes its finite-size dependence from a monotonic increase to a decrease. Moreover, the cusp-like singularity in the momentum dependence at $p = p_3(M)$ is washed out and the spectral weight in (4.1)

is shifted from low to higher excitation energies.

Therefore, we find a further confirmation of the hypothesis formulated in [23]—namely, that field-dependent soft modes only exist if the system is sufficiently frustrated. As was pointed out in [23] this condition is not satisfied in the two-dimensional spin-$\frac{1}{2}$ antiferromagnetic Heisenberg model with nearest-neighbour coupling.

References

[1] Haldane F D M 1982 *Phys. Rev.* B **25** 4925 (erratum 1982 *Phys. Rev.* B **26** 5257)
[2] Tonegawa T and Harada I 1987 *J. Phys. Soc. Japan* **56** 2153
Tonegawa T and Harada I 1988 *Proc. Int. Conf. on Magnetism; J. Physique Coll. Suppl.* **49** C8 1411
[3] Igarashi J and Tonegawa T 1989 *Phys. Rev.* B **40** 756
Igarashi J and Tonegawa T 1989 *J. Phys. Soc. Japan* **58** 2147
[4] Kuboki K and Fukuyama H 1987 *J. Phys. Soc. Japan* **56** 3126
[5] Affleck I, Gepner D, Schulz H J and Ziman T 1989 *J. Phys. A: Math. Gen.* **22** 511
[6] Tonegawa T and Harada I 1987 *J. Phys. Soc. Japan* **56** 2153
Tonegawa T and Harada I 1988 *Proc. Int. Conf. on Magnetism; J. Physique Coll. Suppl.* **49** C8 1411
[7] Tonegawa T, Harada I and Igarashi J 1990 *Prog. Theor. Phys. Suppl.* **101** 513
[8] Tonegawa T, Harada I and Kaburagi M 1992 *J. Phys. Soc. Japan* **61** 4665
[9] Okamoto K and Nomura K 1992 *Phys. Lett.* **169A** 433
[10] Majumdar C K and Ghosh D K 1969 *J. Math. Phys.* **10** 1388
Majumdar C K 1970 *J Phys. C: Solid State Phys.* **3** 911
[11] Eggert S 1996 *Phys. Rev.* B **54** 9612
[12] Schmidt M, Gerhardt C, Mütter K-H and Karbach M 1996 *J. Phys.: Condens. Matter* **8** 553
[13] Yang C N and Yang C P 1966 *Phys. Rev.* **150** 321
Yang C N and Yang C P 1966 *Phys. Rev.* **150** 327
[14] Marshall W 1955 *Proc R. Soc.* A **232** 48
[15] Fledderjohann A, Gerhardt C, Mütter K-H, Schmitt A and Karbach M 1996 *Phys. Rev.* B **54** 7168
[16] Schmidt M 1996 *PhD Thesis* University of Wuppertal
[17] Cardy J L 1986 *Nucl. Phys.* B **270** 186
[18] Schultz H J and Ziman T 1986 *Phys. Rev.* B **33** 6545
[19] Bogoliubov N M, Izergin A G and Korepin V E 1986 *Nucl. Phys.* B **275** 687
[20] Bogoliubov N M, Izergin A G and Reshetikhin N Y 1987 *J. Phys. A: Math. Gen.* **20** 5361
[21] Fledderjohann A, Karbach M, Mütter K-H and Wielath P 1995 *J. Phys.: Condens. Matter* **7** 8993
[22] Viswanath V S, Zhang S, Stolze J and Müller G 1994 *Phys. Rev.* B **49** 9702
Viswanath V S and Müller G 1994 *The Recursion Method—Application to Many Body Dynamics (Springer Lecture Notes in Physics 23)* (New York: Springer)
[23] Yang M S and Mütter K H 1997 *Z. Phys.* at press